

Small angle neutron scattering study on the salt-induced phase separation of 1-propanol aqueous solution

K. Yoshida

Graduate School of Science and Technology, Niigata University, Niigata 950-2181, Japan

M. Misawa^{a)} and K. Maruyama

Department of Chemistry, Faculty of Science, Niigata University, Niigata 950-2181, Japan

M. Imai

Department of Physics, Ochanomizu University, Tokyo 112-0012, Japan

M. Furusaka

Institute of Materials Structure Science, KEK, Tsukuba 305-0801, Japan

(Received 7 December 1999; accepted 9 May 2000)

Small angle neutron scattering (SANS) measurements have been carried out over a wide range of Q from 0.003 to 7 \AA^{-1} on the 1-propanol-water solution with KCl and that without KCl in relation to the salt-induced reentrant phase-separation phenomena. The Q dependence of the SANS intensity for both solutions is characterized by the same fractal structure with the fractal dimension d_f of 1.9. The only difference between the two solutions is the value of correlation length ξ . In the solution without KCl the value of ξ is rather small, ranging from 7.4 to 6.2 \AA depending on temperature, while in the solution with KCl it becomes very large, from 48 to 355 \AA or more depending on temperature, and diverges toward the phase-separation temperatures in a similar way for both the upper and lower one-phase regions. No significant differences have been found on the growing structure of fluctuation in the upper and lower one-phase regions. © 2000 American Institute of Physics. [S0021-9606(00)50730-2]

I. INTRODUCTION

Water and 1-propanol can mix in any proportion at any temperature between 0 and 100 °C. However, when a small amount of salt such as KCl is added into the solution, the phase separation occurs at a finite temperature range¹ confined between a lower phase-separation temperature T_1 and upper one T_h . Below T_1 and above T_h the solution remains in one phase. Figure 1 shows an example of such a phase diagram¹ for the solution with a ratio of water/1-propanol of 5/1 in mole or the mole fraction of 1-propanol c_p of 0.167.

Hayashi and co-workers² studied the solution without KCl by means of small angle x-ray scattering and reported the values of concentration fluctuation $N\langle(\Delta c_p)^2\rangle$ and Debye's correlation lengths L_D as a function of c_p , both of which have maxima at around $c_p=0.2$. Grossmann and Ebert³ also studied this solution by means of photon correlation spectroscopy. Both studies clearly showed the existence of the concentration fluctuation in this solution. However, the details of the concentration fluctuation are still controversial.

We are interested in the salt-induced phase-separation phenomena of this system from a microscopic point of view, especially the role of salt. We carried out small angle neutron scattering measurements on the solution without KCl and the solution with KCl at the temperature below T_1 and above T_h . We intend to examine (1) the mesoscale structure of these solutions, (2) structural evolution toward the phase-

separation temperatures and (3) whether any difference exists in mesoscale structures between the lower and upper one-phase regions.

II. EXPERIMENT

Two solutions were examined: one is the water-1-propanol solution (a ratio of water/1-propanol is 5/1 in mole), denoted as WP hereafter, and another is the solution with the same water/1-propanol ratio as WP but containing 0.0208 mole fraction of KCl, denoted as WPK hereafter. The heavy water D_2O instead of H_2O and a partially D/H substituted 1-propanol C_3H_7OD were used so that one could get a large contrast between the water and 1-propanol molecules in a neutron scattering measurement. Because the D/H substitution shifts the phase-separation temperature slightly from that given in Fig. 1 due to the isotope effect, the amount of KCl added in the $D_2O-C_3H_7OD$ solution was adjusted so as to give the phase-separation temperatures (visually observed) of $T_1 \approx 34$ and $T_h \approx 66$ °C which are suitable for the present neutron scattering instruments.

The small angle neutron scattering measurements were carried out by using a WINK spectrometer installed at the pulsed neutron source KENS, Tsukuba, and SANS-U spectrometer installed at the reactor source JRR3-M, Tokai. Both WINK and SANS-U were used for the measurement at the lower one-phase region, and SANS-U was used for the measurement at the upper one-phase region.

The WINK covers the $Q(=4\pi \sin \theta/\lambda)$ range between 0.03 and 7 \AA^{-1} . The thickness of the sample in the scattering

^{a)} Author to whom correspondence should be addressed.

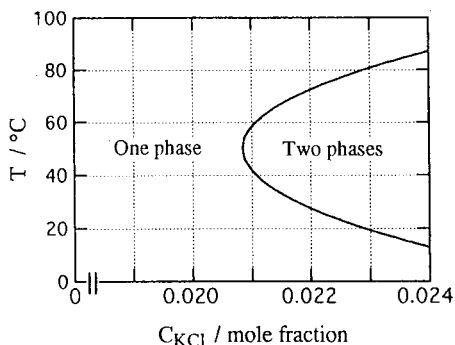


FIG. 1. Salt-induced phase-separation phenomena observed in water-1-propanol solution (the ratio of $\text{H}_2\text{O}/1\text{-C}_3\text{H}_7\text{OH}$ is 5/1 in mole). C_{KCl} is the concentration of KCl added into the solution (Ref. 1).

cell made of silica glass was 2 mm. The scattering intensity $I(Q)$ was obtained from the measured data corrected for self absorption and scattering from the cell by using the TOF (time of flight) analysis program.

While the SANS-U covers the Q range between 0.003 and 0.06 \AA^{-1} , the neutron beam with wavelength of 7 \AA , monochromated mechanically by a velocity selector, was collimated to diameter of 3 mm. The wavelength uncertainty, $\Delta\lambda/\lambda$, was about 10% in this experiment. The camera distance was 8 m for the measurement of WPK solution and was 2 m for the WP solution. The scattered neutrons were detected by the position sensitive detector, the resolution of which was $5 \times 5 \text{ mm}$. The scattering intensity $I(Q)$ was obtained from the measured two-dimensional data corrected for self absorption and scattering from the cell. The thickness of the sample in the scattering cell made of silica glass was also 2 mm.

The measurements of $I(Q)$ for the solution of WPK were carried out as a function of temperature by increasing the temperature in the lower one-phase region, while the measurements were carried out by decreasing the temperature in the upper one-phase region. The temperature of the sample was kept within $0.1 \text{ }^\circ\text{C}$ during each measurement. The measurement of temperature dependence of $I(Q)$ for the solution WP was also carried out by increasing temperature.

III. RESULTS

Figure 2 shows the scattered intensities $I(Q)$ over the wide range of Q from 0.003 to 7 \AA^{-1} , which are obtained by combining the data measured by both spectrometers WINK and SANS-U at the region of Q of $0.03\text{--}0.04 \text{ \AA}^{-1}$. The curves (A) show the intensities $I(Q)$ for the solution of WP which does not include KCl. The intensity at low Q region below 1 \AA^{-1} of these curves increases clearly, indicating that the concentration fluctuation occurs even in the solution without salt, which is in good agreement with the previous x-ray² and light³ scattering results.

The curves (B) show the $I(Q)$ for the solution of WPK which includes KCl. The scattering intensity at low Q region increases significantly by the addition of KCl, which is two or three orders of magnitude larger than that of the solution WP. The temperature of $37 \text{ }^\circ\text{C}$ is close to the lower phase separation temperature, while the temperature of $25 \text{ }^\circ\text{C}$ is far

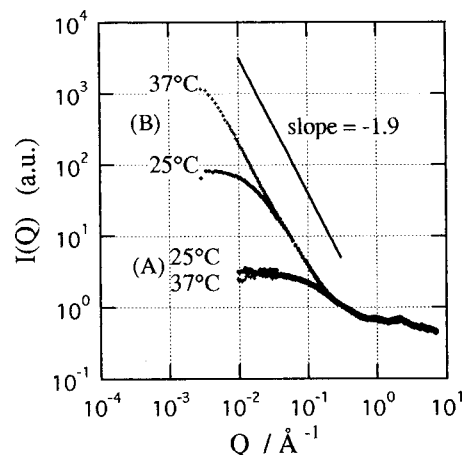


FIG. 2. Typical example of SANS intensity $I(Q)$ measured by using SANS-U and WINK spectrometers. Curves (A) show the $I(Q)$ measured for the solution without KCl, while curves (B) the solution with KCl.

below that temperature. The plot of $\log I(Q)$ vs $\log Q$ of this solution at $37 \text{ }^\circ\text{C}$ is almost linear at a range of Q between 5×10^{-3} and $2 \times 10^{-1} \text{ \AA}^{-1}$ and the slope is about -1.9 as shown in Fig. 2, suggesting the fractal nature of the fluctuation.

Figure 3 shows the temperature dependence of $I(Q)$ for the solution WP measured at various temperatures between 25 and $80.1 \text{ }^\circ\text{C}$ by using SANS-U. The intensity decreases with increasing temperature. We also carried out the temperature dependence of $I(Q)$ for the solution WPK at various temperatures between 20 and $37 \text{ }^\circ\text{C}$ in the lower one-phase region and between 63 and $76 \text{ }^\circ\text{C}$ in the upper one-phase region by using SANS-U, which are discussed in Sec. IV.

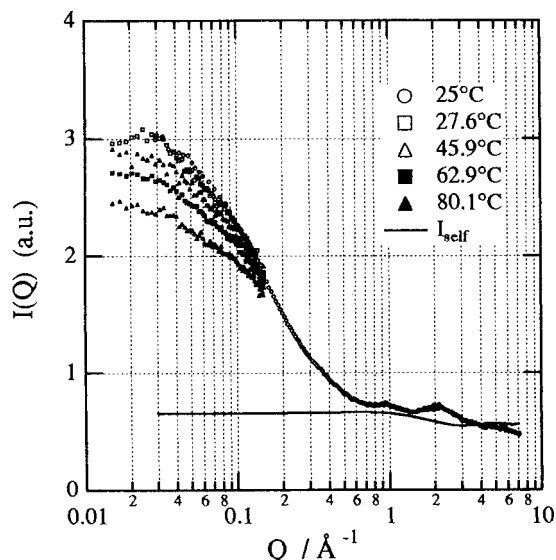


FIG. 3. Temperature dependence of $I(Q)$ measured by using SANS-U for the solution without KCl. $I(Q)$ measured by using WINK at $25 \text{ }^\circ\text{C}$ is also plotted for $Q > 0.03 \text{ \AA}^{-1}$. A solid line shows the scattering intensity $I_{\text{self}}(Q)$ given by Eq. (13).

IV. DISCUSSION

A. Scattering function

Because the mesoscale structure of the present solution is characterized by fractal as suggested in Sec. III, we analyze the $I(Q)$ data based on the fractal model. The mesoscale structure depends mainly on the scattering-density distribution and not on any details of the structure in molecular level such as orientational correlation between molecules. Therefore, the following formula of $I(Q)$ for the mixture of uncorrelated molecules is suitable for the present purpose, which is a simple extension of the formula for a monatomic binary liquid.^{4,5}

$$I(Q) = \alpha[\langle f_1(Q) \rangle - \langle f_u^2(Q) \rangle + \langle f_u(Q) \rangle^2 S_{NN}(Q) + 2\langle f_u(Q) \rangle (\Delta f_u(Q)) S_{NC}(Q) + (\Delta f_u(Q))^2 S_{cc}(Q) + \langle I_{inc}/4\pi \rangle], \quad (1)$$

where

$$\begin{aligned} \langle f_1(Q) \rangle &= c_p f_{1p}(Q) + c_w f_{1w}(Q) \\ &= c_p \sum_p b_i b_{ij_0}(Q r_{ij}) + c_w \sum_w b_i b_{ij_0}(Q r_{ij}), \end{aligned} \quad (2)$$

$$\begin{aligned} \langle f_u(Q) \rangle &= c_p f_{up}(Q) + c_w f_{uw}(Q) \\ &= c_p \sum_p b_i j_0(Q r_{i0}) + c_w \sum_w b_i j_0(Q r_{i0}), \end{aligned} \quad (3)$$

$$\langle f_u^2(Q) \rangle = c_p f_{up}^2(Q) + c_w f_{uw}^2(Q), \quad (4)$$

$$\Delta f_u(Q) = f_{up}(Q) - f_{uw}(Q), \quad (5)$$

$$I_{inc} = c_p I_{inc,p} + c_w I_{inc,w}, \quad (6)$$

$\langle f_1(Q) \rangle$ is an averaged intramolecular scattering intensity, $\langle f_u(Q) \rangle$ an averaged intermolecular form factor, $\langle I_{inc} \rangle$ an averaged incoherent scattering cross section, $c_w (= 1 - c_p)$ a concentration of water molecules, b_i a coherent scattering length of atom i , r_{ij} an intramolecular distance between i and j atoms, r_{i0} a distance between atom i and a molecular center, $j_0(x)$ a spherical Bessel function of 0th order. The summation \sum_p (\sum_w) is made over all atoms in a 1-propanol (water) molecule. $S_{NN}(Q)$, $S_{NC}(Q)$ and $S_{cc}(Q)$ are number-number, number-concentration, and concentration-concentration correlation functions, respectively. The equation (1) has the correct asymptotic forms at both limits of $Q \rightarrow 0$ and $Q \rightarrow \infty$.

If one assumes that the Q dependence of the dilatation factor $\Delta(Q)$ and the compressibility factor $\theta(Q)$ defined in Ref. 5 is small, which may be suitable for the low Q region we are interested in, and both factors can be replaced by the values at $Q=0$, that is $\Delta(0) = -\delta[-(V_p - V_w)/\langle V \rangle]$ and $\theta(0) = \rho_m k T \kappa_T$ (where ρ_m is a molecular number density and κ_T an isothermal compressibility), then Eq. (1) is simplified for the low Q region as^{4,5}

$$I(Q) = \alpha[\langle f_1(Q) \rangle - \langle f_u^2(Q) \rangle + \langle f_u(Q) \rangle^2 \rho_m k T \kappa_T + (\langle f_u(Q) \rangle \delta - \Delta f_u(Q))^2 S_{cc}(Q) + \langle I_{inc}/4\pi \rangle], \quad (7)$$

Furthermore, in the present case the contribution of the concentration fluctuation, the fourth term in Eq. (7), is predominant compared to that of the number fluctuation $\langle f_u(Q) \rangle^2 \rho_m k T \kappa_T$, because $\langle f_u(0) \rangle^2 \rho_m k T \kappa_T$ is evaluated to be 0.14 barns with $\langle f_u(0) \rangle^2 = 3.12$ barns and $\kappa_T = 530 \text{ TPa}^{-1}$,⁶ which is negligibly small compared to (44 to 33) barns for the fourth term $(\langle f_u(0) \rangle \delta - \Delta f_u(0))^2 S_{cc}(0)$ with $(\langle f_u(0) \rangle \delta - \Delta f_u(0))^2 = 22.0$ barns and $S_{cc}(0) = (2.0 \text{ to } 1.5)$ which is shown later. Then Eq. (7) can be rewritten as

$$I(Q) = \alpha[\langle f_1(Q) \rangle - \langle f_u^2(Q) \rangle + (\langle f_u(Q) \rangle \delta - \Delta f_u(Q))^2 S_{cc}(Q) + \langle I_{inc}/4\pi \rangle]. \quad (8)$$

$S_{cc}(Q)$ is related to the partial pair distribution functions^{4,5} $g_{pp}(r)$, $g_{ww}(r)$ and $g_{pw}(r)$, which are propanol-propanol, water-water and propanol-water pair distribution functions, respectively,

$$S_{cc}(Q) = c_p c_w \left[1 + c_p c_w \int 4\pi r^2 \rho_m (g_{pp}(r) + g_{ww}(r) - 2g_{pw}(r)) \frac{\sin Qr}{Qr} dr \right]. \quad (9)$$

As suggested in Sec. III, the $I(Q)$ has a fractal nature, which means that $[g_{pp}(r) + g_{ww}(r) - 2g_{pw}(r)]$ may have a characteristic form for a fractal structure given by⁷

$$\rho_m (g_{pp}(r) + g_{ww}(r) - 2g_{pw}(r)) = \frac{A}{r^{d-d_f}} \exp\left(-\frac{r}{\xi}\right), \quad (10)$$

where d_f is a fractal dimension, ξ a correlation length and A a constant. The Fourier transform of Eq. (10) is given by⁷

$$S_{fr}(Q) = \frac{C(d_f - 1)\Gamma(d_f - 1)\xi^{d_f} (1 + Q^2\xi^2)^{1/2}}{(1 + Q^2\xi^2)^{d_f/2}} \frac{1}{Q\xi} \times \frac{\sin[(d_f - 1)\arctan(Q\xi)]}{d_f - 1}, \quad (11)$$

where Γ is the gamma function, and C a constant.

Substituting the above equation into Eqs. (9) and (8), we have

$$I(Q) = \alpha[\langle f_1(Q) \rangle - \langle f_u^2(Q) \rangle + c_p c_w (\langle f_u(Q) \rangle \delta - \Delta f_u(Q))^2 + c_p^2 c_w^2 (\langle f_u(Q) \rangle \delta - \Delta f_u(Q))^2 S_{fr}(Q) + \langle I_{inc}/4\pi \rangle]. \quad (12)$$

We examine the Q dependence of the observed $I(Q)$ based on the fractal model given by Eq. (12).

B. The solution without KCl; WP

From Eq. (12), the scattering intensity $I_{self}(Q)$, which is independent of fractal structure, is given by Eq. (13),

$$I_{self}(Q) = \alpha[\langle f_1(Q) \rangle - \langle f_u^2(Q) \rangle + c_p c_w (\langle f_u(Q) \rangle \delta - \Delta f_u(Q))^2 + \langle I_{inc}/4\pi \rangle], \quad (13)$$

and is shown in Fig. 4(a) by a solid curve. The value of α is estimated so that the $I_{self}(Q)$ coincides with the observed $I(Q)$ at the higher Q region. However, because the observed

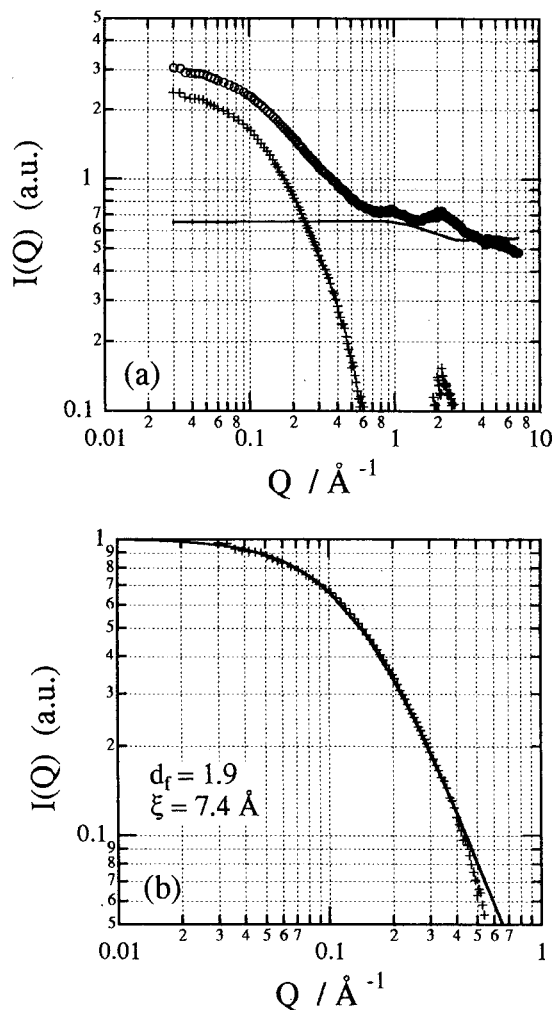


FIG. 4. (a) Scattering intensity $I_{\text{self}}(Q)$ (solid line) given by Eq. (13) is subtracted from experimental $I(Q)$ (open circles) for the solution without KCl at 25 °C. Residue is plotted by plus marks. (b) Comparison of residual $I(Q)$ (plus) with that for fractal model calculated by Eq. (11) with $d_f = 1.9$ and $\xi = 7.4 \text{ \AA}$ (solid line).

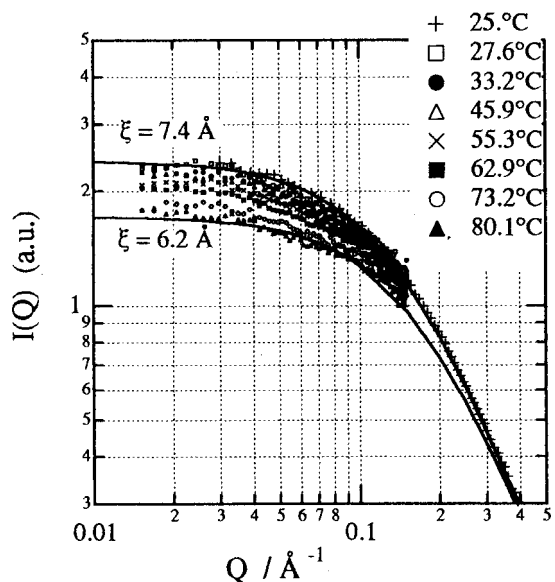


FIG. 5. Comparison of residual $I(Q)$ measured at elevated temperature (marks) and those calculated for fractal model with two typical values of ξ (solid lines). Fractal dimension is obtained to be 1.9 despite temperature.

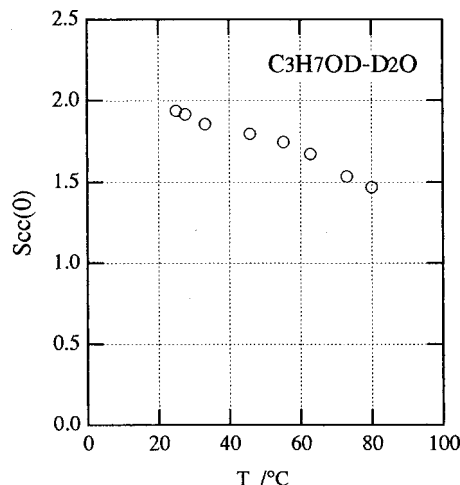


FIG. 6. Temperature dependence of $S_{cc}(0)$ estimated for the solution without KCl.

intensity at the higher Q region decreases gradually due to the recoil effect, the estimated value of α has some ambiguity. Nevertheless, we think that the estimated value of α is good enough for the present purpose. We subtract $I_{\text{self}}(Q)$ from the observed intensity measured at 25 °C and obtained the residue which is shown by plus marks in Fig. 4(a).

The residue is compared with the scattering intensity based on the fractal model by using Eqs. (11) and (12). Because $f_{up}(Q)$ and $f_{uw}(Q)$ are almost constant in a range of Q less than 1 \AA^{-1} , we may neglect any Q dependence of $(\langle f_u(Q) \rangle \delta - \Delta f_u(Q))^2$ in the present analysis and put it at constant in the following analysis. The residue is fitted very well by the fractal model as shown in Fig. 4(b) by a solid curve with a fractal dimension d_f of 1.9 and correlation length ξ of 7.4 Å. The slight discrepancy of the fitted curve from the observed one at $Q > 0.4 \text{ \AA}^{-1}$ may be due to the effect of excluding volume of finite size of molecules⁷ and/or neglecting the Q dependence of $(\langle f_u(Q) \rangle - \delta \Delta f_u(Q))^2$ and ambiguity in α . The fitted results for $I(Q) - I_{\text{self}}(Q)$ at elevated temperatures are shown in Fig. 5. The fractal dimen-

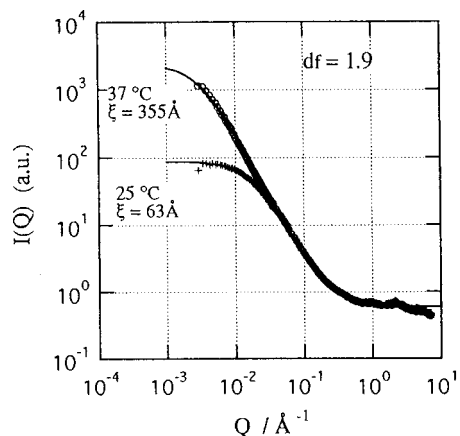


FIG. 7. Comparison of experimental and calculated $I(Q)$ for solution with KCl. Curves fitted by using Eq. (12) are shown by solid lines. Fractal dimension obtained is 1.9, which is independent of temperature.

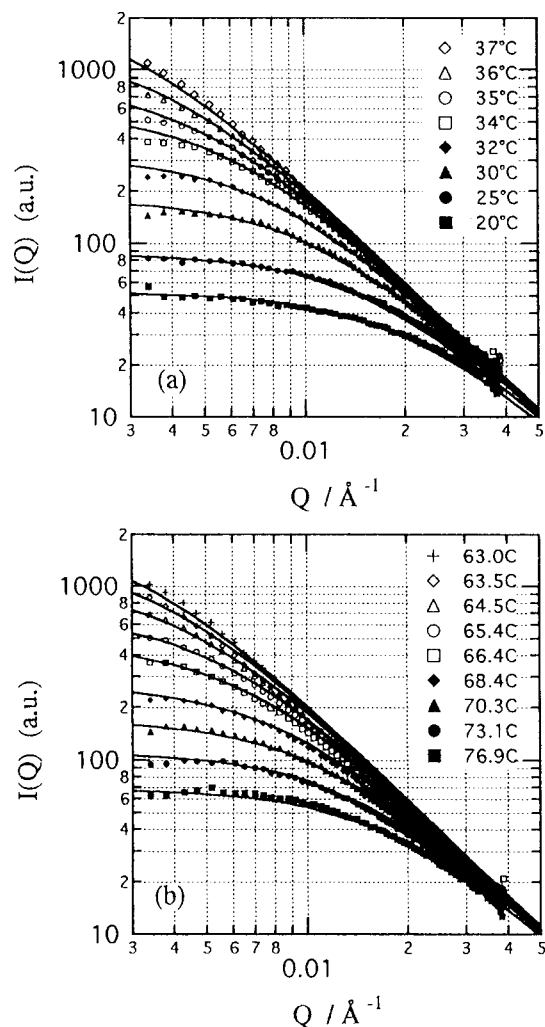


FIG. 8. Comparison of temperature dependence of $I(Q)$ measured by SANS-U (marks) and fitted ones (solid lines) by using Eq. (12) for solution with KCl at lower one-phase region (a), and upper one-phase region (b).

sion estimated is $d_f=1.9$ regardless of temperature, while the correlation length ξ decreases gradually to 6.2 \AA with increasing temperature.

The temperature dependence of $S_{cc}(0)$ evaluated by Eq. (8) is plotted in Fig. 6. The value of $S_{cc}(0)$ decreases with increasing temperature.

C. The solution with KCl; WPK

Similarly we fit the intensities observed for the solution with KCl, WPK, based on the fractal model described above. The results fitted to Eq. (12) are shown by solid curves in Fig. 7. The experimental data measured at 25 and 37°C are fitted very well over the full range of Q studied. Both fits give the same value 1.9 for the fractal dimension d_f regardless of temperature, the value of which is also the same as that for the solution without KCl.

Figures 8(a) and 8(b) show the similar fits to the intensities measured at various temperatures in the lower and upper one-phase regions. All curves are fitted very well by the fractal model and again the same value of $d_f=1.9$ is obtained despite the lower and upper one-phase regions.

Figure 9(a) shows the correlation length ξ estimated by

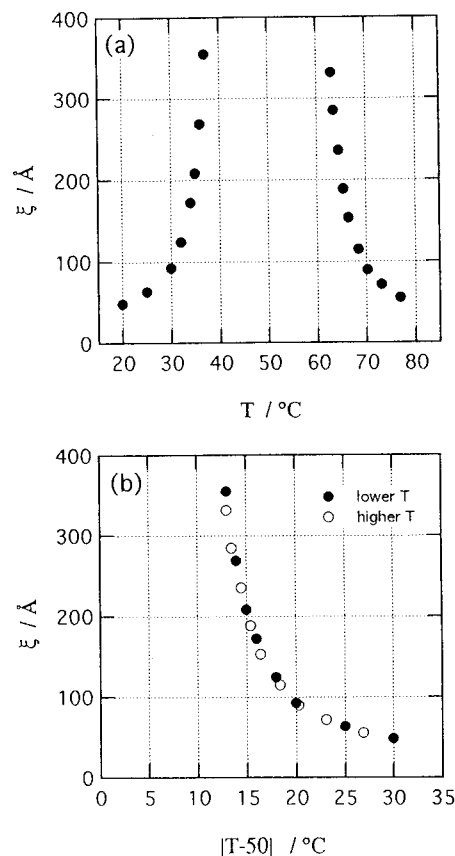


FIG. 9. (a) Temperature dependence of correlation length ξ estimated for solution with KCl. (b) Plot of ξ vs $|T(^{\circ}\text{C}) - 50|$.

the present fit as a function of temperature. The value of ξ diverges toward the critical temperatures which are slightly inside of the two-phase boundary. Furthermore, the temperature dependence of ξ in the lower and upper one-phase regions is quite similar if one plots the ξ as a function of $|T(^{\circ}\text{C}) - 50|$ as shown in Fig. 9(b). This suggests that the same mechanism may act for the salt-induced phase separation in this solution despite the lower and upper one-phase regions.

V. CONCLUSION

The analysis of SANS intensity measured for the solution without KCl shows the fractal nature of the concentration fluctuation with a fractal dimension d_f of 1.9. The correlation length ξ decreases slightly with increasing temperature from 7.4 \AA at 25°C to 6.2 \AA at 80.1°C.

The SANS intensity measured for the solution with KCl increases significantly by two or three orders of magnitude larger than that of the solution without KCl. The characteristic Q dependence of the intensity is analyzed also by the fractal structure, which gives the same fractal dimension d_f of 1.9 as obtained for the solution without KCl. This value of 1.9 is independent of temperature studied for both the lower and upper one-phase regions. The value of 1.9 is close to that obtained for the fractal structure of the cluster-cluster aggregation.⁸ However, we are not sure at present the details of the structure of current fluctuation. The correlation length ξ increases significantly by the addition of salt and depends

strongly on temperature, and diverges toward the critical temperatures in a similar way in both the upper and lower one-phase regions. We find no significant differences in the growth of mesoscale structure in the upper and lower one-phase regions as far as the SANS measurements are concerned.

We summarize that the concentration fluctuation of both solutions with KCl and without KCl have the same fractal nature with $d_f=1.9$. The only difference is the value of correlation length ξ . The addition of small amounts of salt increases the value of ξ significantly but does not affect the fractal nature of the fluctuation. This suggests that the fluctuation grows up largely without changing its fractal structure by the addition of a small amount of salt. The microscopic role of the salt on growing the fluctuation and leading to the phase separation is still an open question. It is suggested, however, that the mechanism for the salt-induced phase separation seems to be the same in the lower and upper one-phase regions.

ACKNOWLEDGMENT

A part of this work was supported by the Ministry of Education, Science and Culture of Japan, under Grant No. 07236104.

¹G. M. Schneider, *Ber. Bunsenges. Phys. Chem.* **76**, 325 (1972).

²H. Hayashi, K. Nishikawa, and T. Iijima, *J. Phys. Chem.* **94**, 8334 (1990).

³G. H. Grossman and K. H. Ebert, *Ber. Bunsenges. Phys. Chem.* **85**, 1026 (1981).

⁴F. J. Pearson and G. S. Rushbrooke, *Proc. R. Soc. Edinburgh, Sect. A: Math. Phys. Sci.* **64**, 303 (1957).

⁵A. B. Bhatia and D. E. Thornton, *Phys. Rev. B* **2**, 3004 (1970).

⁶O. Kiyohara and G. C. Benson, *J. Solution Chem.* **10**, 281 (1981).

⁷T. Freltoft, K. Kjems, and S. K. Sinha, *Phys. Rev. B* **33**, 269 (1986).

⁸J. F. Gouyet, *Physics and Fractal Structures* (Masson, Paris, 1996), p. 131.